# Endogenous miR-204 Protects the Kidney against Chronic Injury in Hypertension and Diabetes

Yuan Cheng,[1,2,3] Dandan Wang,[2,3,4] Feng Wang,[3,5] Jing Liu,[3] Baorui Huang,[3,5] Maria Angeles Baker,[3] Jianyong Yin,[5] Rui Wu,[5] Xuanchen Liu,[5] Kevin R. Regner,[6] Kristie Usa,[3] Yong Liu,[3] Congxiao Zhang,[7] Lijin Dong,[7] Aron M. Geurts,[3] Niansong Wang,[5] Sheldon S. Miller,[7] Yongcheng He,[8] and Mingyu Liang[3]

Due to the number of contributing authors, the affiliations are listed at the end of this article.

## ABSTRACT

**Background** Aberrant microRNA (miRNA) expression affects biologic processes and downstream genes that are crucial to CKD initiation or progression. The miRNA miR-204-5p is highly expressed in the kidney but whether miR-204-5p plays any role in the development of chronic renal injury is unknown.

**Methods** We used real-time PCR to determine levels of miR-204 in human kidney biopsies and animal models. We generated *Mir204* knockout mice and used locked nucleic acid–modified anti-miR to knock down miR-204-5p in mice and rats. We used a number of physiologic, histologic, and molecular techniques to analyze the potential role of miR-204-5p in three models of renal injury.

**Results** Kidneys of patients with hypertension, hypertensive nephrosclerosis, or diabetic nephropathy exhibited a significant decrease in miR-204-5p compared with controls. Dahl salt-sensitive rats displayed lower levels of renal miR-204-5p compared with partially protected congenic SS.13$^{BN26}$ rats. Administering anti–miR-204-5p to SS.13$^{BN26}$ rats exacerbated interlobular artery thickening and renal interstitial fibrosis. In a mouse model of hypertensive renal injury induced by uninephrectomy, angiotensin II, and a high-salt diet, *Mir204* gene knockout significantly exacerbated albuminuria, renal interstitial fibrosis, and interlobular artery thickening, despite attenuation of hypertension. In diabetic db/db mice, administering anti–miR-204-5p exacerbated albuminuria and cortical fibrosis without influencing blood glucose levels. In all three models, inhibiting miR-204-5p or deleting *Mir204* led to upregulation of protein tyrosine phosphatase SHP2, a target gene of miR-204-5p, and increased phosphorylation of signal transducer and activator of transcription 3, or STAT3, which is an injury-promoting effector of SHP2.

**Conclusions** These findings indicate that the highly expressed miR-204-5p plays a prominent role in safeguarding the kidneys against common causes of chronic renal injury.

*JASN* 31: 1539–1554, 2020. doi: https://doi.org/10.1681/ASN.2019101100

CKD represents a substantial disease burden worldwide. CKD manifests as reduced kidney function and progressive renal damage. The asymptomatic nature and lack of effective diagnosis at the early stage of the disease predispose the patients to high risk of developing ESKD and cardiovascular complications. Diabetes and hypertension are two leading causes of CKD and ESKD worldwide.[1–3] The prevalence of diabetes is increasing, which contributes to an increase of patients with CKD and ESKD. The renal pathologies caused by diabetes include thickening of glomerular basement membrane,

Received October 23, 2019. Accepted April 9, 2020.

Y.C., D.W., and F.W. contributed equally to this work.

Published online ahead of print. Publication date available at www.jasn.org.

**Correspondence:** Dr. Mingyu Liang, Center of Systems Molecular Medicine, Department of Physiology, Medical College of Wisconsin, 8701 Watertown Plank Road, Milwaukee, WI 53226, or Dr. Yongcheng He, Department of Nephrology, Shenzhen Hengsheng Hospital, 20 Yintian Rd, Shenzhen, Guangdong, People's Republic of China. E-mail: mliang@mcw.edu or heyongcheng@medmail.com.cn

mesangial expansion, nodular sclerosis, and advanced diabetic glomerulosclerosis.[4] As the second common cause of CDK and ESKD, hypertensive renal injury is characterized as hypertensive nephrosclerosis, which may include arteriolosclerosis, interstitial inflammation and fibrosis, tubular atrophy and loss, and lesions of FSGS.[5]

MicroRNAs (miRNAs) are a group of small noncoding RNAs approximately 22 nucleotides long that have important roles in the post-transcriptional regulation of their target gene expression.[6,7] Approximately 2000 miRNAs that are predicted to regulate a majority of protein-coding genes have been identified in humans.[8] A variety of miRNAs are specifically abundant in the kidney and the dysregulation of miRNAs is associated with the development of several kidney diseases.[6,9–13] Aberrant miRNA expression plays an important role in CKD by affecting multiple biologic processes and downstream genes that are critical to disease initiation or progression.[14–17]

We previously performed a small RNA deep-sequencing analysis of human kidney biopsy specimens from patients diagnosed with hypertensive nephrosclerosis.[18] The miRNA miR-204-5p exhibited the largest downregulation among all miRNAs detected. miR-204-5p also is one of the most abundantly expressed miRNAs in these human kidneys. However, the functional role of miR-204-5p in the kidney is largely unknown. In this study, we further analyzed the expression of miR-204-5p in human kidney biopsy specimens from people with hypertensive or diabetic injury and investigated the functional significance of endogenous miR-204-5p in the development of hypertensive and diabetic renal injury and the molecular mechanisms involved in three animal models.

**Significance Statement**

Several microRNAs have been shown to play significant roles in the development of renal injury. The microRNA miR-204-5p is highly enriched in the kidney but its involvement in chronic renal injury is unknown. In this study, the authors report that miR-204-5p abundance is significantly decreased in kidney biopsy samples from patients with hypertension, hypertensive nephrosclerosis, or diabetic nephropathy. They also found, in a rat model of salt-sensitive hypertension, a mouse model of hypertension, and a mouse model of type 2 diabetes, inhibition of miR-204-5p, or deletion of the *Mir204* gene results in upregulation of an injurious molecular pathway and substantial exacerbation of renal injury. These findings provide evidence of a prominent role for miR-204-5p in safeguarding the kidneys against common causes of chronic renal injury.

## METHODS

### Human Kidney Biopsy Samples

Protocols involving the use of human materials and medical information for miR-204-5p measurements were approved by the Institutional Review Board at Shanghai Jiao Tong University Affiliated Sixth People's Hospital. Records at the pathologic archive at Shanghai Jiao Tong University Affiliated Sixth People's Hospital from 2015 to 2017 were searched to identify subjects diagnosed with hypertensive nephrosclerosis or diabetic nephropathy without any other type of renal injury and control subjects diagnosed with minimal or no renal injury (Supplemental Table 1). The hypertension group of subjects were further divided into those who were hypertensive with or without nephrosclerosis. The control subjects were biopsied because of hematuria with or without mild albuminuria. The control subjects did not have hypertension or diabetes. Kidney biopsy blocks were cut into 10-$\mu$m sections. Total RNA was extracted from three sections from each subject using the miRNeasy FFPE Kit (Qiagen) as described previously.[19]

### *In Situ* Hybridization

*In situ* hybridization (ISH) was performed on formalin-fixed, paraffin-embedded sections of human kidney biopsy specimens using carboxyfluorescein-labeled probes (Servio Tech, Wuhan, China) for miR-204-5p and scrambled control as described previously.[20] Briefly, tissue sections (5 $\mu$m) were cleared in xylenes and rehydrated using an ethanol gradient. The sections were then exposed to 30 minutes of proteinase K (20 mg/ml) treatment at 37°C. After 1 hour of prehybridization buffer treatment at 37°C, the sections were incubated with the probe (concentration 8 ng/$\mu$l) at 40°C overnight. After washing, the slides were developed with 4′,6-diamidino-2-phenylindole solution in the dark for 8 minutes to stain the nucleus. Images were captured with fluorescence microscopy (Eclipse Ti-SR, Nikon, Japan). 4′,6-Diamidino-2-phenylindole signals were examined with excitation wavelength 330–380 nm and emission wavelength 420 nm. Carboxyfluorescein signals were examined with excitation wavelength 465–495 nm and emission wavelength 515–555 nm.

### Rat Model of Hypertensive Renal Injury

All experimental procedures involving animals were approved by the Institutional Care and Use Committee of the Medical College of Wisconsin or Shanghai Jiao Tong University Affiliated Sixth People's Hospital. Male salt-sensitive (SS) and congenic SS-13$^{BN26}$ rats were generated as described previously.[21,22] All rats were bred and housed in an American Association for Accreditation of Laboratory Animal Care–accredited animal care facility at the Medical College of Wisconsin with free access to water and a custom AIN-76A purified rodent chow containing 0.4% sodium chloride (NaCl) (Dyets, Bethlehem, PA).[23,24] Experiments were performed on 6-week-old male rats. A gel-filled catheter attached to a BP telemetry transmitter (Data Sciences International) was implanted into the right carotid artery for chronic measurement of BP as described previously.[25,26] BP data were collected, stored, and analyzed using Dataquest A.R.T. 4.0 software (Data Sciences International). After a 7-day recovery period and 3 days of stable baseline BP recording, rats were switched to a high-salt diet containing 4.0% NaCl for 14 days before the rats were euthanized for tissue collection.

### Generation of *Mir204* Knockout Mice

*Mir204* gene knockout mice were generated using a bacterial artificial chromosome–based targeting vector to delete the entire coding sequence of *Mir204*. The presence of the targeted allele was determined by long-range PCR, followed by Southern blotting. See Results for characterization of this knockout model. The mouse colony was maintained using heterozygous *Mir204*$^{+/-}$ breeders.

### Mouse Model of Hypertensive Renal Injury

The left kidney was removed from the mouse at the age of 9 weeks and telemeters (model PA-C10; Data Sciences International) were implanted in the right carotid artery at the age of 10 weeks. The procedure of recovery, BP recording, food change, and tissue collection was similar to the protocol for rats. Angiotensin II (Ang II) was subcutaneously infused for 14 days at a dose of 1 $\mu$g/kg per minute by osmotic minipump (Alzet 1002; Durect Corporation) after 3 days of baseline BP recording.[27,28] Mice were switched to the 4% NaCl diet when the Ang II infusion was initiated.

### Mouse Model of Diabetic Nephropathy

Db/db mice, provided by Nanjing Institute of Biomedicine, were used as a model of type 2 diabetes and diabetic nephropathy. Db/m mice were used as control for db/db mice. Anti-miR treatment was started at 12 weeks of age as described below. Urine samples were collected every 2 weeks. Tissues were collected at 24 weeks of age.

### *In Vivo* Administration of anti-miR

Locked nucleic acid (LNA)–modified anti-miR was used to knock down specific miRNAs *in vivo*, in a manner similar to that reported previously.[14] Rats received intraperitoneal injections of LNA anti–miR-204-5p or LNA-scrambled anti-miR at 2 mg/kg just before the initiation of the high-salt diet and then again after 7 days on the high-salt diet. Db/db mice received intraperitoneal injections of LNA anti–miR-204-5p or LNA-scrambled anti-miR at 2 mg/kg once a week for 12 weeks.

### RNA Extraction and Quantitative Real-Time PCR

Total RNA was purified from animal tissue specimens using the chloroform/TRIzol method according to the manufacturer's protocol. miR-204-5p abundance was quantified using a TaqMan miRNA Assay Kit (catalog number 4440887, assay identifier 000508; Life Technologies) as described before.[29] RNU6B (catalog number 4440887, assay identifier 001093; Life Technologies) or 5S ribosomal RNA was used as the normalizer. Real-time PCR analysis for mRNA was performed using SYBR Green chemistry as described previously.[30,31] $\beta$-Actin or 18S ribosomal RNA was used as the internal normalizer. Sequences of custom-designed primers are shown in Supplemental Table 2.

### Western Blot

Protein extraction and Western blot analysis were performed as previously described.[29,32] The primary antibodies used were rabbit anti–phosphorylated signal transducer and activator of transcription 3 (anti–p-Stat) mAb (#9145, dilution 1:1000; Cell Signaling Technology) and mouse anti-Stat3 mAb (#9139, dilution 1:1000; Cell Signaling Technology). The secondary antibodies were goat anti-rabbit IgG–horseradish peroxidase (sc-2004, dilution 1:10,000; Santa Cruz Biotechnology) and goat anti-mouse IgG–horseradish peroxidase (sc-2005, dilution 1:10,000; Santa Cruz Biotechnology). Coomassie Blue staining was used to normalize the abundance of specific proteins.

### Histologic and Immunohistochemical Analysis

The collected kidney was fixed with a 10% buffered formalin solution. Kidneys were paraffin embedded and 3-$\mu$m sections were mounted. Sections were stained with Masson trichrome stain to highlight the casts and the fibrotic tissue as previously described.[20,33] Stained slides were scanned by NanoZoomer digital pathology scanner and analyzed blindly using MetaMorph image analysis software. Approximately ten to 15 interlobular arteries were included from a randomly chosen section, and the average was used for statistical analysis. The total vascular area and lumen area of interlobular arteries were measured and wall/lumen area ratio was calculated to determine the relative median wall thickness as described previously.[33,34] Interstitial fibrosis and tubular casts were determined by quantifying the area of extracellular matrix protein–containing tissue or the blocked tubules filled with protein as a percentage of total tissue area.[20,33,35] Mesangial matrix index was estimated as described previously.[36] Immunohistochemistry analysis was performed on formalin-fixed, paraffin-embedded sections of kidneys following the procedures we described previously.[20,33] Kidney sections were immunostained with anti–p-Stat3 (#9145, dilution 1:200; Cell Signaling Technology) and anti-Stat3 (#9139, dilution 1:200; Cell Signaling Technology).

### Biochemical Assays

Urinary albumin was quantified using an Albumin Blue 580 (Molecular Probes) fluorescence assay following the manufacturer's protocol. Serum creatinine was measured using a commercial kit (#65340; Abcam) and blood glucose was monitored using a glucose meter (Accu-Chek; Roche). Activated STAT3 (p-STAT3) in tissue or cell lysate was measured using an ELISA kit (#126458; Abcam). Src activity (phospho-Src) was measured with an ELISA kit (Raybiotech, Norcross, GA).

### Statistical Analysis

Results are expressed as mean±SEM. Data were analyzed using *t* test or one-way or two-way ANOVA followed by Holm–Šidák *post hoc* test. A $P$ value $<0.05$ was considered statistically significant.

## RESULTS

### miR-204-5p Levels Are Lower in Kidney Biopsies from Patients with Hypertension, Hypertensive Nephrosclerosis, or Diabetic Nephropathy

The abundance of miR-204-5p was measured with real-time PCR in kidney biopsy specimens from patients with

hypertension or hypertensive nephrosclerosis, as well as patients with diabetic nephropathy. Kidney biopsy samples without overt histologic pathologies were used as controls. Clinical characteristics of patients with hypertension or hypertensive nephrosclerosis have been described previously.[18] The average BP levels of the last three visits in the hypertension group (systolic/diastolic BP, 142±4/87±2 mm Hg; $n=8$) and hypertensive nephrosclerosis group (144±3/90±3 mm Hg; $n=32$) were higher than that in the control group (114±2/73±1 mm Hg; $n=10$; $P<0.05$). Urinary albumin-creatinine ratios were 225±36 mg/g in controls, 195±58 mg/g in the hypertension group, and 444±69 mg/g in the hypertensive nephrosclerosis group. Demographic and clinical characteristics of patients with diabetic nephropathy are shown in Supplemental Table 1.

miR-204-5p was downregulated in kidneys of patients with hypertension or hypertensive nephrosclerosis (Figure 1A), as well as in patients with diabetic nephropathy (Figure 1B), compared with their control human subjects. In the hypertension study (Figure 1A), miR-204-5p is decreased in both hypertensive groups regardless of the presence of hypertensive nephrosclerosis, which suggests the decrease of miR-204-5p in hypertension might precede overt renal injury. The minor strand miR-204-3p was not detectable in these biopsy specimens using real-time PCR. ISH analysis indicated that miR-204-5p was widely expressed in glomeruli and tubules in human kidneys (Figure 1C). miR-204-5p signals appeared to decrease in the glomeruli in the patients compared with control human subjects. However, the signals were not completely lost in any cell type and the ISH analysis was not sufficiently quantitative to definitively identify cell types in which miR-204-5p expression was downregulated in the patients.

## Knockdown of miR-204-5p Exacerbates Renal Injury in SS.13$^{BN26}$ Rats Fed a High-Salt Diet

We used animal models to test the hypothesis that endogenous miR-204-5p is protective against chronic renal injury. The Dahl SS rat is a commonly used model of human SS forms of hypertension and renal injury.[37,38] The SS.13$^{BN26}$ rat is a congenic strain that was derived from the SS rat and develops substantially milder SS hypertension and renal injury.[21,22,39] miR-204-5p abundance was measured in the renal cortex of SS rats and SS.13$^{BN26}$ rats that were maintained on a 0.4% NaCl diet or had been switched to a 4% NaCl diet for 3 or 7 days. miR-204-5p abundance was significantly lower in SS rats compared with SS.13$^{BN26}$ rats treated with

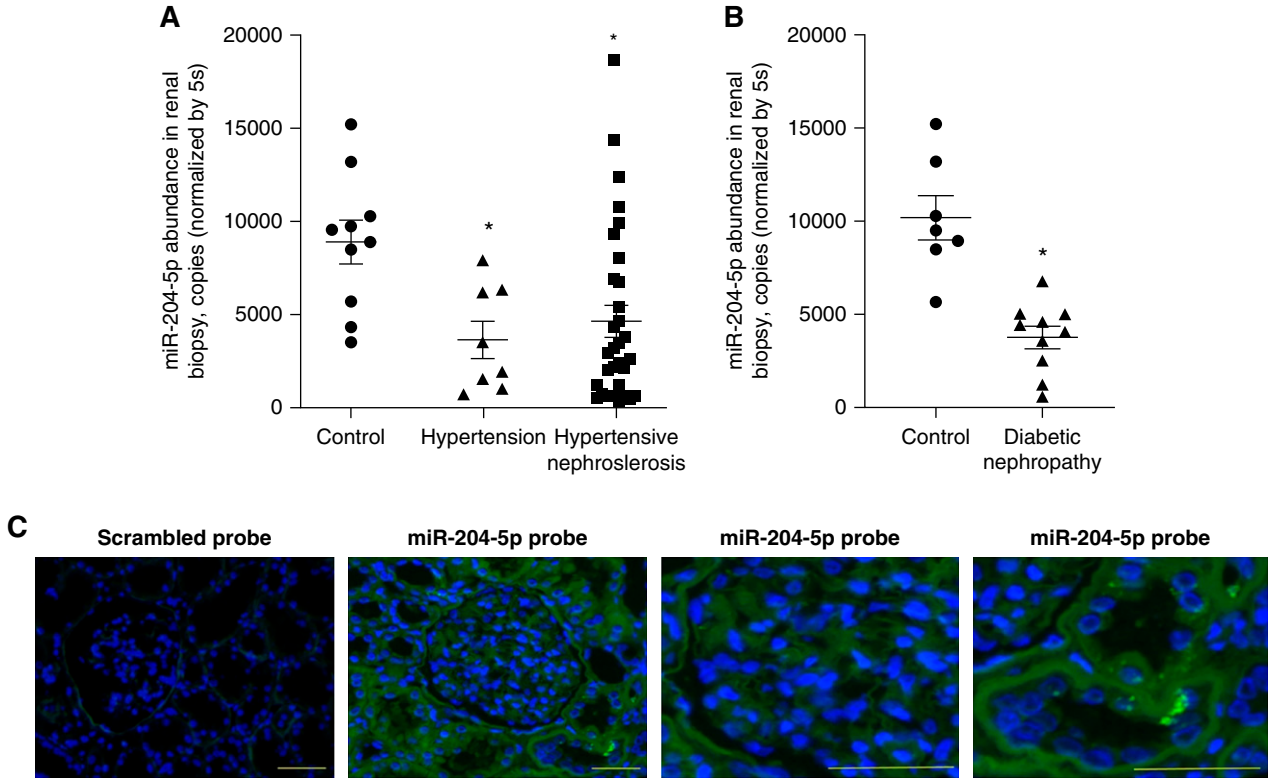


**Figure 1.** miR-204-5p is downregulated in kidneys of patients with hypertension, hypertensive nephrosclerosis, or diabetic nephropathy. miR-204-5p abundance was measured in human kidney biopsy specimens using quantitative PCR or detected using ISH. (A) Renal miR-204-5p abundance in hypertension and hypertensive nephrosclerosis. $n=10$ for control, $n=8$ for hypertension, and $n=32$ for hypertensive nephrosclerosis. *$P<0.05$, versus control, one-way ANOVA followed by Holm–Šidák *post hoc* test. (B) Renal miR-204-5p abundance in diabetic nephropathy. $n=7$ for control and $n=10$ for diabetic nephropathy. *$P<0.05$, versus control, *t* test. (C) Representative ISH images in kidney biopsy from a control subject. Zoomed-in images with miR-204-5p probe show miR-204-5p expression in a glomerulus and tubules. Scale bar, 100 $\mu$m.

the 4% NaCl diet for 7 days (Figure 2A), suggesting the higher level of miR-204-5p in SS.13$^{BN26}$ might protect the rats from salt-induced hypertension or renal injury as compared with SS rats. To examine this possibility, LNA-modified scrambled anti-miR or anti–miR-204-5p oligonucleotide was administered to SS.13$^{BN26}$ rats by intraperitoneal injection. The detectable abundance of miR-204-5p in the renal cortex and outer medulla was significantly lower in the anti–miR-204-5p group compared with the scrambled anti-miR group (Figure 2B). Mean arterial pressure (MAP) was increased by approximately 15 mm Hg compared

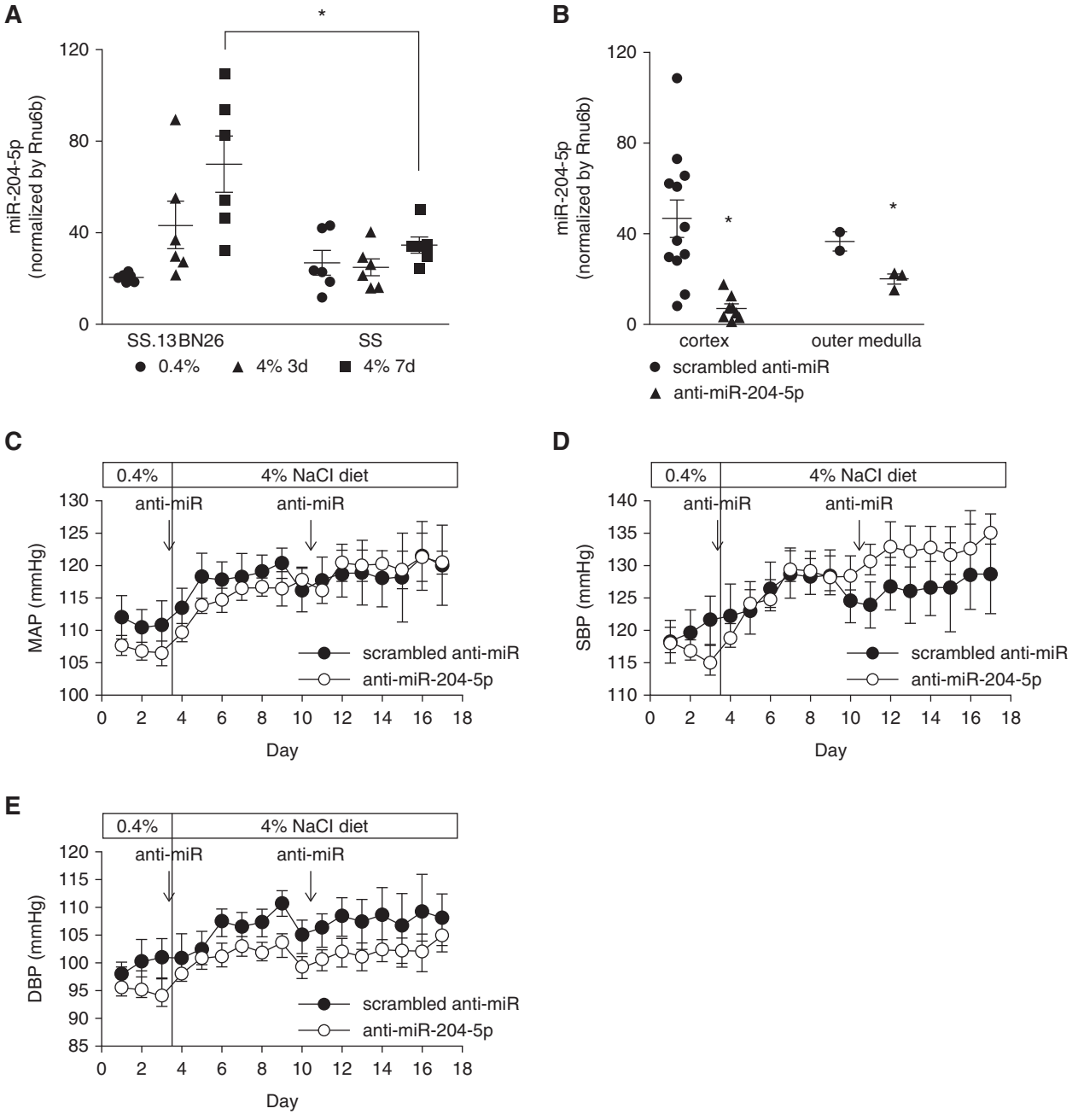


**Figure 2.** Knockdown of miR-204-5p did not significantly influence the development of modest hypertension in SS.13$^{BN26}$ rats fed a high-salt diet. (A) miR-204-5p abundance in the renal cortex in SS rats compared with protected SS.13$^{BN26}$ rats fed a 4% NaCl diet for 3 or 7 days ($n$=6/group). *$P$<0.05, two-way ANOVA followed by Holm–Šidák test. (B) miR-204-5p abundance in the kidneys of SS.13$^{BN26}$ rats treated with anti–miR-204-5p. For renal cortex, $n$=12 in scrambled anti-miR group, $n$=9 in anti–miR-204-5p group. For renal outer medulla, $n$=3 per group. *$P$<0.05 compared with scrambled anti-miR group, $t$ test. (C–E) Mean arterial BP (MAP), systolic BP (SBP), and diastolic BP (DBP) in SS.13$^{BN26}$ rats fed a 4% NaCl diet. Scrambled anti-miR or anti–miR-204-5p was injected intraperitoneally at 2 mg/kg body wt on the days indicated by the arrows. $n$=12 in scrambled anti-miR group, $n$=9 in anti–miR-204-5p group.

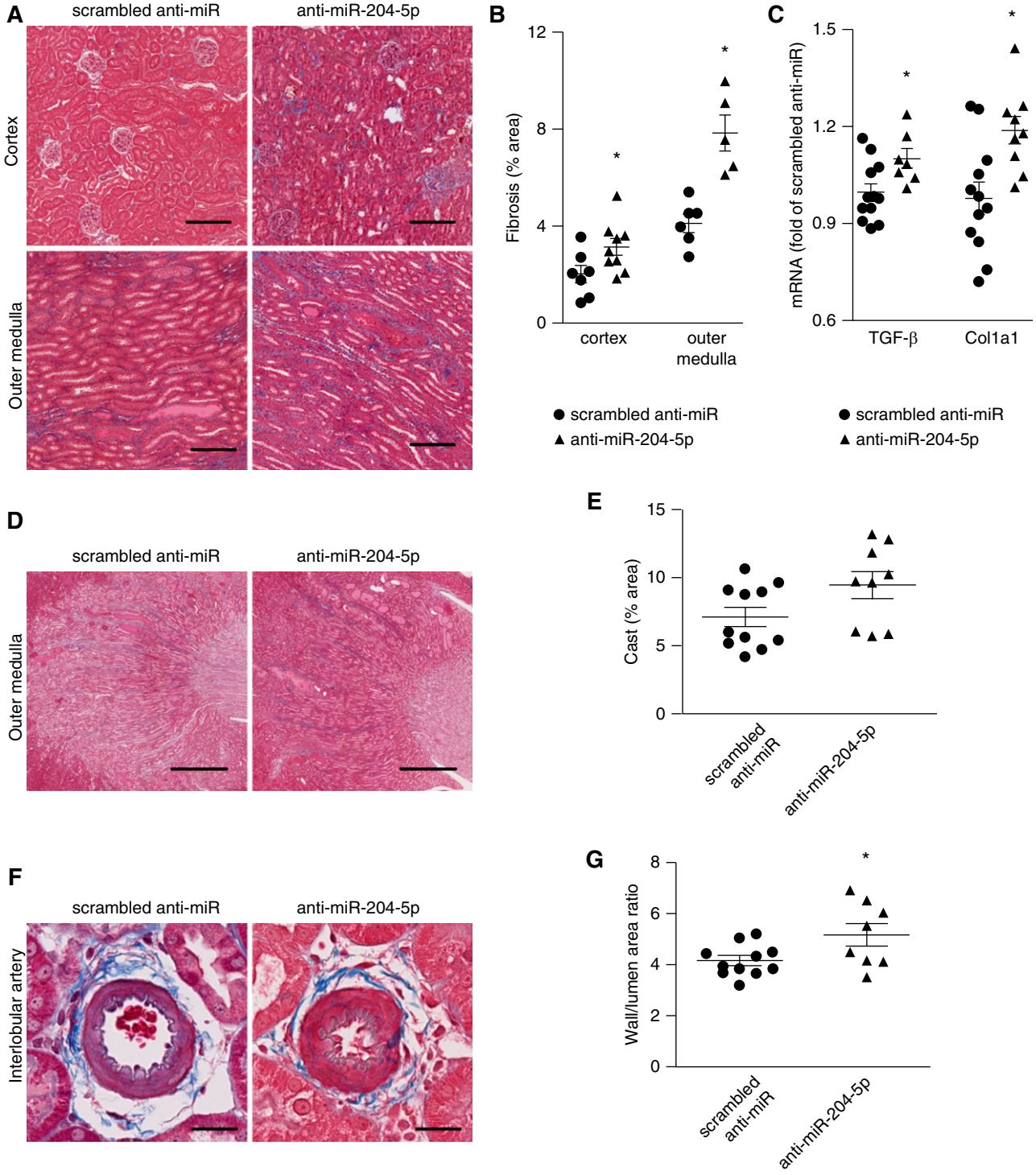


**Figure 3.** Knockdown of miR-204-5p exacerbates renal injury in SS.13$^{BN26}$ rats fed a high-salt diet. (A) Representative kidney sections with trichrome staining showing interstitial fibrosis (blue) in the cortex and outer medulla of SS.13$^{BN26}$ rats at the end of the treatment protocol shown in Figure 2B. Scale bar, 200 $\mu$m; original magnification, ×100. (B) Area of interstitial fibrosis, based on trichrome staining, as percentage of total kidney section area. $n$=12 in scrambled anti-miR group, $n$=9 in anti–miR-204-5p group. *$P$<0.05, compared with scrambled, $t$ test. (C) TGF-$\beta$ and COL1A1 mRNA abundance in the renal cortex normalized to $\beta$-actin and expressed as fold of the average level in the scrambled anti-miR group. $n$=12 in scrambled anti-miR group, $n$=9 in anti–miR-204-5p group. *$P$<0.05, compared with scrambled. (D) Representative trichrome staining of kidney sections showing cast in tubules of outer medulla. Scale bar, 1000 $\mu$m; original magnification, ×25; $t$ test. (E) The blocked tubules filled with protein (red) content was quantitated in the outer medulla and expressed as percentage of total area. $n$=12 in scrambled anti-miR group, $n$=9 in anti–miR-204-5p group, $P$=0.05, $t$ test.

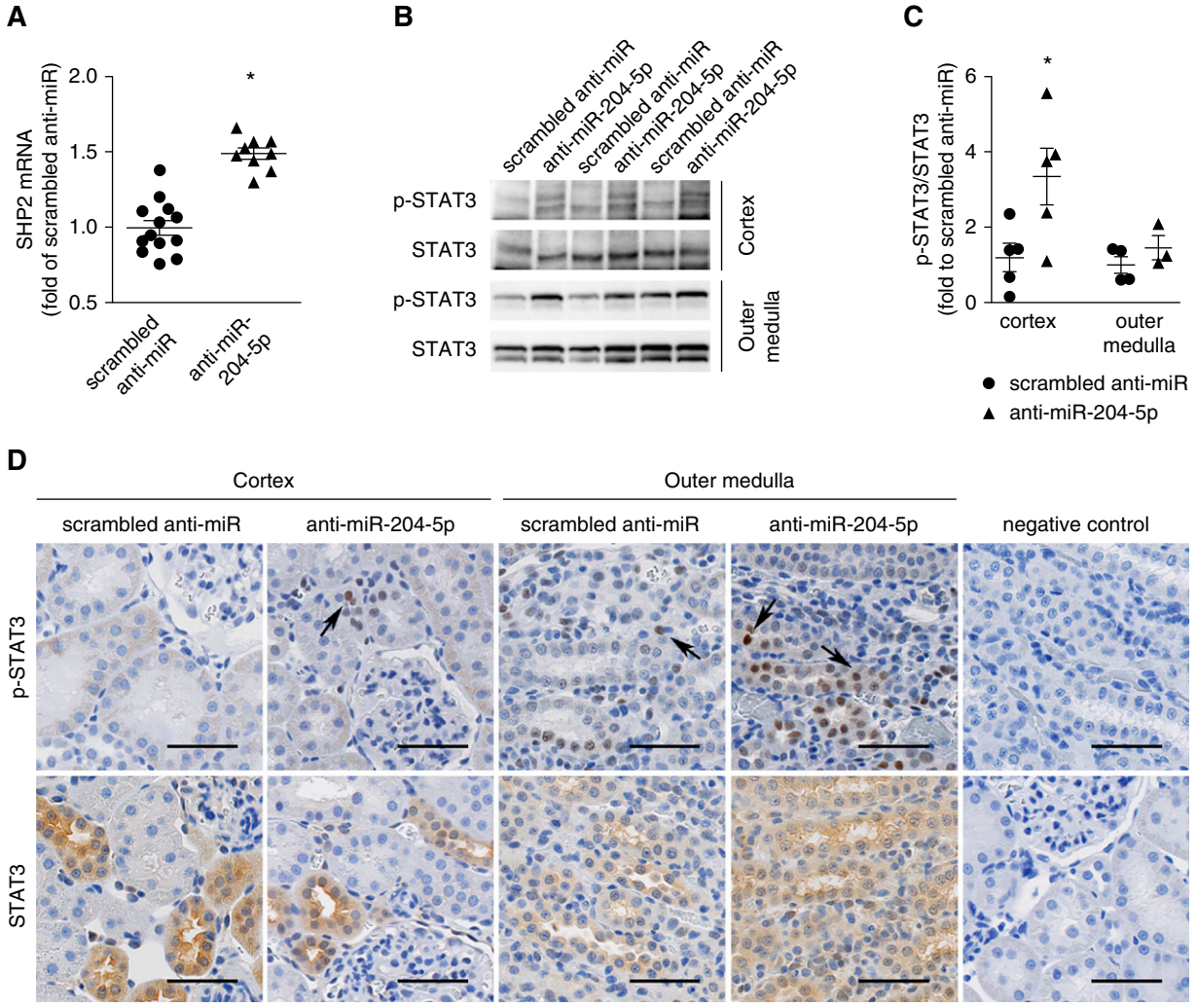


**Figure 4.** Knockdown of miR-204-5p leads to upregulation of SHP2 and p-STAT3 in SS.13$^{BN26}$ rats. (A) SHP2 mRNA was quantified with real-time PCR in the renal cortex at the end of the treatment protocol shown in Figure 2B and expressed as fold of the average level in the scrambled anti-miR group. $n=12$ in scrambled anti-miR group, $n=9$ in anti–miR-204-5p group. *$P<0.05$, compared with scrambled anti-miR group, *t* test. (B) Western blot analysis of STAT3 and p-STAT3 in kidney tissues at the end of the treatment protocol shown in Figure 2B, *t* test. (C) Quantification of p-STAT3/STAT3 ratios based on Western blot and expressed as fold of the average ratio in the scrambled anti-miR group. $n=12$ in scrambled anti-miR group, $n=9$ in anti–miR-204-5p group. *$P<0.05$, compared with scrambled group, *t* test. (D) Representative photomicrographs of immunohistochemistry analysis of STAT3 and p-STAT3 in kidneys at the end of treatment protocol shown in Figure 2B. Primary antibody was omitted in the negative control. Scale bar, 50 $\mu$m; image magnification, 20 ×. Arrows point to representative nuclei stained positive for p-STAT3.

with the baseline in both groups after the rats were switched to the 4% NaCl diet for 2 weeks (Figure 2C). Knockdown of miR-204-5p did not significantly influence salt-induced changes in MAP, systolic pressure, or diastolic pressure (Figure 2, C and D).

We next examined the kidneys for histologic features of renal injury including fibrosis and thickening of arterial walls. Trichrome staining showed knockdown of miR-204-5p significantly exacerbated fibrosis in the renal cortex and outer medulla (Figure 3, A and B). TGF-$\beta$ is a central contributor to renal fibrosis. Collagen type I accumulation is a hallmark of renal fibrosis. Real-time PCR analysis showed that the expression of TGF-$\beta$ and collagen type I $\alpha$1 (COL1A1) were

(F) Representative trichrome staining of kidney sections showing interlobular arteries. Scale bar, 25 $\mu$m; original magnification, ×400. (G) The wall/lumen area ratio of interlobular artery. $n=12$ in scrambled group, $n=9$ in anti–miR-204-5p group. *$P<0.05$ compared with scrambled anti-miR group, *t* test.

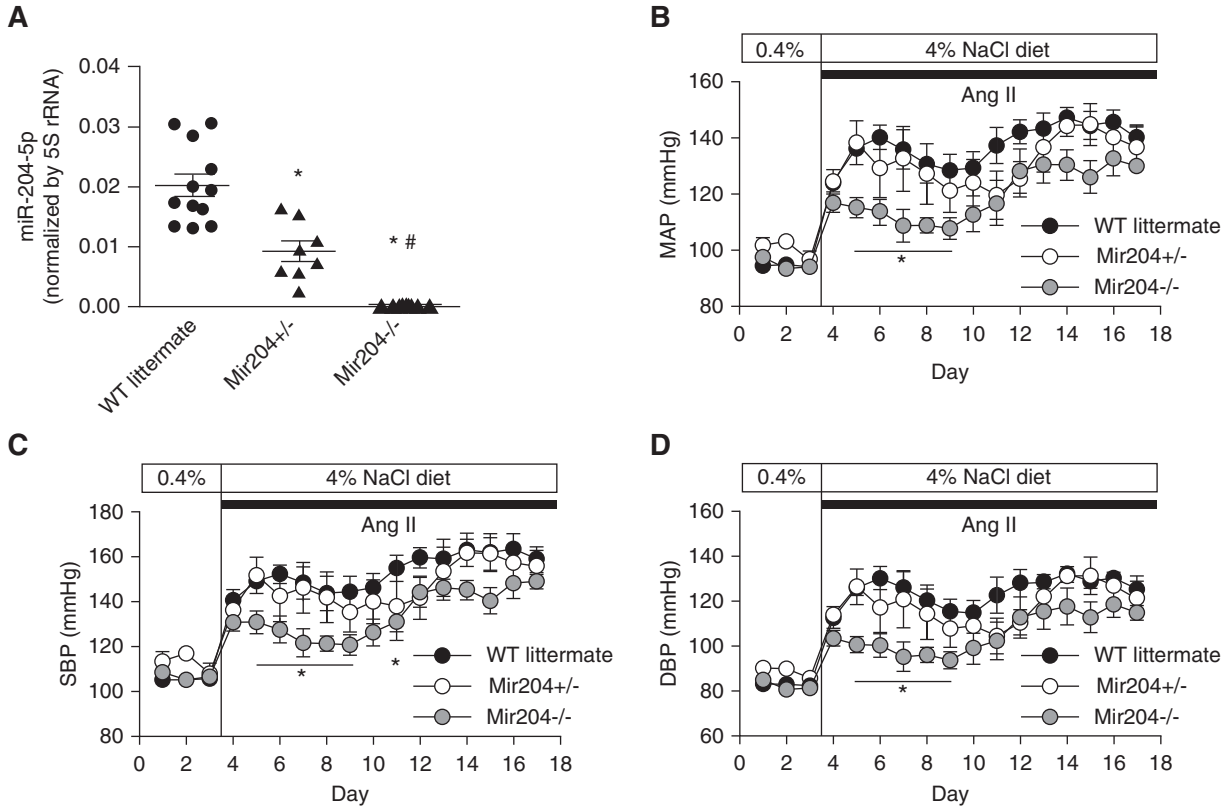


**Figure 5.** *Mir204* knockout delays the development of hypertension in uninephrectomized mice treated with Ang II and a high-salt diet. (A) miR-204-5p abundance in renal cortex from *Mir204*$^{-/-}$ ($n$=10), *Mir204*$^{+/-}$ ($n$=8), and wild-type (WT) littermate ($n$=12) mice using real-time PCR. *$P$<0.001 versus wild type, #$P$<0.001 versus *Mir204*$^{+/-}$, one-way ANOVA followed by Holm–Šidák test. (B–D) MAP, systolic BP (SBP), and diastolic BP (DBP) in *Mir204*$^{-/-}$ ($n$=10), *Mir204*$^{+/-}$ ($n$=8), and WT littermate ($n$=12) mice. *$P$<0.05 compared with WT littermates at the same time points, two-way repeated measure ANOVA followed by Holm–Šidák test.

significantly elevated in the kidneys of the anti–miR-204-5p group (Figure 3C). The tubular cast region of the outer medulla tended to be larger in the anti–miR-204-5p group than in the scrambled anti-miR group (Figure 3, D and E). Proteinuria was not significantly different between the two groups (12.0±1.4 versus 11.0±1.5 mg total protein/mg creatinine; NS).

The wall/lumen ratio of interlobular artery was significantly increased in the anti–miR-204-5p group, which is a salient feature of hypertensive renal injury (Figure 3, F and G). The difference in the wall/lumen ratio between the treated and control groups was approximately 25%, which is substantial. Previous studies reported differences of approximately 15% in the wall/lumen ratio between kidneys in SS rats exposed to up to a 40 mm Hg difference in perfusion pressure for 2 weeks.[33]

Together, these data indicated that knockdown of miR-204-5p exacerbated renal injury in SS.13$^{BN26}$ rats that developed modest hypertension on a high-salt diet.

### Knockdown of miR-204-5p Leads to Upregulation of SHP2 and p-STAT3 in SS.13$^{BN26}$ Rats

Protein tyrosine phosphatase nonreceptor type 11 (SHP2) is a proven, direct target of miR-204-5p.[40] SHP2 can activate the tyrosine kinase Src and STAT3, which is known to contribute to renal interstitial fibrosis.[41–43] SHP2 mRNA abundance and the activities of STAT3 as measured by the ratio of phosphorylated STAT3 over total STAT3 were significantly upregulated in the renal cortex in the anti–miR-204-5p group (Figure 4, A–C). Immunohistochemistry analysis indicated STAT3 was predominantly localized to the cytoplasm with sporadic nuclear staining in the tubulointerstitial compartment. p-STAT3 was mainly localized to the nucleus, which appeared to be increased in the anti–miR-204-5p group (Figure 4D). These data indicated that knockdown of miR-204-5p led to upregulation of SHP2 which might activate the Src-STAT3 pathway in the kidneys of SS.13$^{BN26}$ rats fed the high-salt diet.

### *Mir204* Knockout Exacerbates Renal Injury and Upregulates SHP2/p-STAT3 in Uninephrectomized Mice Treated with Ang II and a High-Salt Diet

We investigated whether miR-204 influenced the development of hypertensive renal injury in models other than the one derived from the SS rat. A mouse model with deletion of the miR-204 coding sequence was developed using classic homologous recombination in mouse embryonic stem cells.[44] In brief, the 68-bp pre-miRNA sequence of murine *Mir204*, the gene coding for both the -5p and -3p strands of miR-204, was

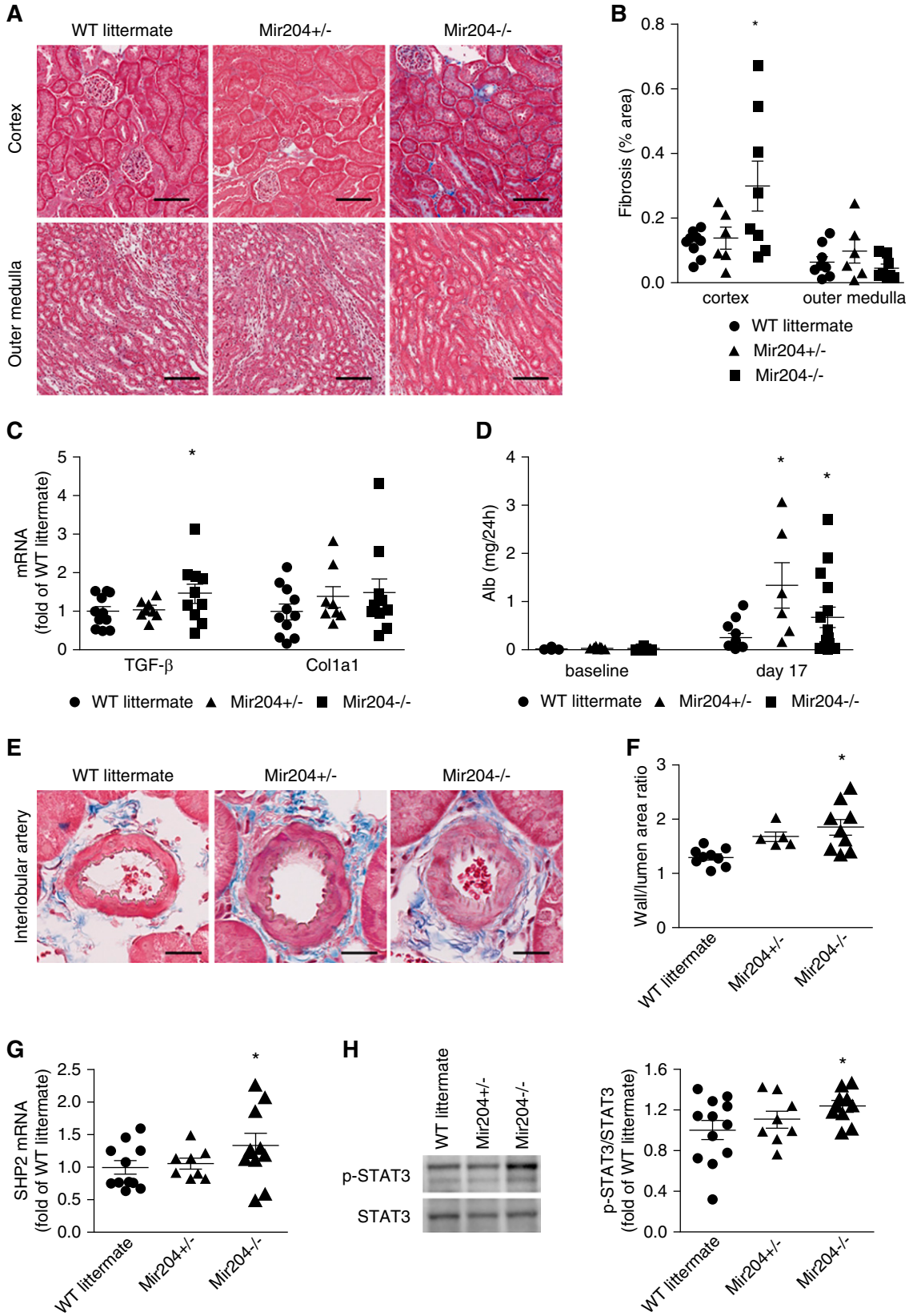


**Figure 6.** *Mir204* knockout exacerbates renal injury and upregulates target SHP2/p-STAT3 pathway in uninephrectomized mice treated with Ang II and a high-salt diet. (A) Representative trichrome staining of kidney sections showing interstitial fibrosis (blue) in

precisely removed to generate the *Mir204* knockout allele ($Mir204^{-/-}$). This allele was subsequently bred into the C57BL/6J background for at least ten generations to reach the congenic state. We confirmed the absence of miR-204-5p in the kidney of $Mir204^{-/-}$ mice and observed significant reduction of miR-204-5p abundance in $Mir204^{+/-}$ mice compared with wild-type littermates (Figure 5A). Changes of miR-204-3p abundance in the knockout mice followed the same pattern as miR-204-5p.

Hypertension and hypertensive renal injury were induced in these mice using uninephrectomy, Ang II, and a high-salt (4% NaCl) diet. C57BL/6J mice are highly resistant to the development of hypertensive renal injury. The combined treatment is necessary to induce renal injury.[45,46] The combined treatment did not significantly change miR-204-5p levels in the renal cortex of wild-type mice ($1.0\pm0.03$ in untreated mice versus $0.92\pm0.04$ in the combined treatment group, $n=4$ and 5, NS). Ang II and the 4% NaCl diet increased MAP by up to approximately 50 mm Hg in uninephrectomized $Mir204^{+/-}$ mice and wild-type littermates over 2 weeks (Figure 5B). The increase of MAP as well as systolic BP and diastolic BP was significantly attenuated in $Mir204^{-/-}$ mice for several days shortly after the initiation of the treatment (Figure 5, B–D).

Renal interstitial fibrosis in these mice was much milder than that in SS.13$^{BN26}$ rats. Nevertheless, $Mir204^{-/-}$ mice had significantly more interstitial fibrosis compared with $Mir204^{+/-}$ and wild-type littermate mice (Figure 6, A and B). Consistent with that, TGF-$\beta$ mRNA abundance was significantly higher in $Mir204^{-/-}$ mice (Figure 6C). COL1A1 mRNA tended to be higher in the knockout mice, but the difference did not reach statistical significance. Albuminuria, an index of renal injury, was increased in all three groups at the end of the 2-week treatment. The increase of albuminuria was significantly exacerbated in $Mir204^{-/-}$ and $Mir204^{+/-}$ mice compared with wild-type littermates (Figure 6D). Serum creatinine levels did not differ significantly between the three genotypes ($0.31\pm0.07$, $0.35\pm0.28$, and $0.23\pm0.03$ mg/dl in $Mir204^{+/+}$, $Mir204^{+/-}$, and $Mir204^{-/-}$ mice, respectively; $n=7$ for each genotype, NS).

The wall/lumen area ratio in interlobular artery was significantly higher in $Mir204^{-/-}$ and $Mir204^{+/-}$ mice compared with wild-type littermates (Figure 6, E and F). The difference between the knockout and wild type was approximately 30%, which, again, was substantial as it was in the case of SS.13$^{BN26}$ rats treated with anti–miR-204-5p. The exacerbation of renal injury, as measured by all of the indexes described above, occurred despite similar or even lower levels of hypertension in $Mir204^{-/-}$ and $Mir204^{+/-}$ mice (Figure 5, B–D).

mRNA abundance of SHP2 was significantly higher in the renal cortex of $Mir204^{-/-}$ mice compared with $Mir204^{+/-}$ and their wild-type littermates (Figure 6G), consistent with SHP2 being a target gene of miR-204-5p. Similar to the findings in the rat model, the activation of STAT3 was significantly enhanced in $Mir204^{-/-}$ mice (Figure 6H).

### Knockdown of miR-204-5p Exacerbates Albuminuria and Renal Injury and Enhances SHP2/p-STAT3 in Diabetic Mice

We next examined the role of endogenous miR-204-5p in the development of chronic kidney injury in diabetic db/db mice, a commonly used mouse model of diabetes and diabetic nephropathy. miR-204-5p levels in the renal cortex were significantly higher in db/db mice compared with control db/m mice ($1.0\pm0.2$ in db/m versus $1.7\pm0.2$ in db/db, $n=5$, $P<0.05$). We administered scrambled anti-miR or anti–miR-204-5p oligonucleotide in db/db mice intraperitoneally once a week for 12 weeks. The anti–miR-204-5p treatment significantly decreased real-time PCR–detectable levels of miR-204-5p in the renal cortex (Figure 7A). Compared with control db/m mice, db/db mice exhibited hyperglycemia and obesity, which were not altered by the anti–miR-204-5p treatment (Figure 7, B and C). Compared with control db/m mice, db/db mice exhibited higher kidney weight and increased

renal cortex and outer medulla at the end of the treatment protocol shown in Figure 5B. Scale bar, 100 $\mu$m; original magnification, $\times$200. (B) Area of interstitial fibrosis, based on trichrome staining, as percentage of total kidney section area. $n=5$ for each group, *$P<0.05$ compared with wild-type (WT) littermates, one-way ANOVA followed by Holm–Šidák test. (C) TGF-$\beta$ and Col1a1 mRNA abundance in the renal cortex normalized to $\beta$-actin and expressed as fold of the average level in the WT littermate group. $n=8$ for $Mir204^{+/-}$ mice, $n=10$ for $Mir204^{-/-}$ mice, and $n=12$ for WT littermates. *$P<0.05$, compared with WT littermates, one-way ANOVA followed by Holm–Šidák test. (D) *Mir204* knockout exacerbates albuminuria in uninephrectomized mice treated with Ang II and a high-salt diet. Shown is 24 hours of urinary albumin excretion. $n=12$, $n=8$, and $n=10$ for WT, $Mir204^{+/-}$, and $Mir204^{-/-}$, respectively. *$P<0.05$ compared with WT littermates, one-way ANOVA followed by Holm–Šidák test. (E) Representative trichrome staining of kidney sections showing interlobular arteries at the end of the treatment protocol shown in Figure 5B. Scale bar, 20 $\mu$m; original magnification, $\times$400. (F) Quantification of the wall/lumen area ratio of interlobular artery. $n=5$ for each group. *$P<0.05$, compared with WT littermates, one-way ANOVA followed by Holm–Šidák test. (G) miR-204-5p target gene SHP2 mRNA was quantified with real-time PCR in the renal cortex at the end of the treatment protocol shown in Figure 5B and expressed as fold of the average level in the WT littermate group. $n=8$ for $Mir204^{+/-}$ mice, $n=10$ for $Mir204^{-/-}$ mice, and $n=12$ for wild-type littermates. *$P<0.05$, compared with WT littermates, one-way ANOVA followed by Holm–Šidák test. (H) Western blot analysis of STAT3 and p-STAT3 in renal cortex at the end of the treatment protocol, and quantification of p-STAT3/STAT3 ratios based on Western blot and expressed as fold of the average ratio in the WT littermate group. $n=8$ for $Mir204^{+/-}$ mice, $n=10$ for $Mir204^{-/-}$ mice, and $n=12$ for wild-type littermates. *$P<0.05$, compared with WT littermates, one-way ANOVA followed by Holm–Šidák test.

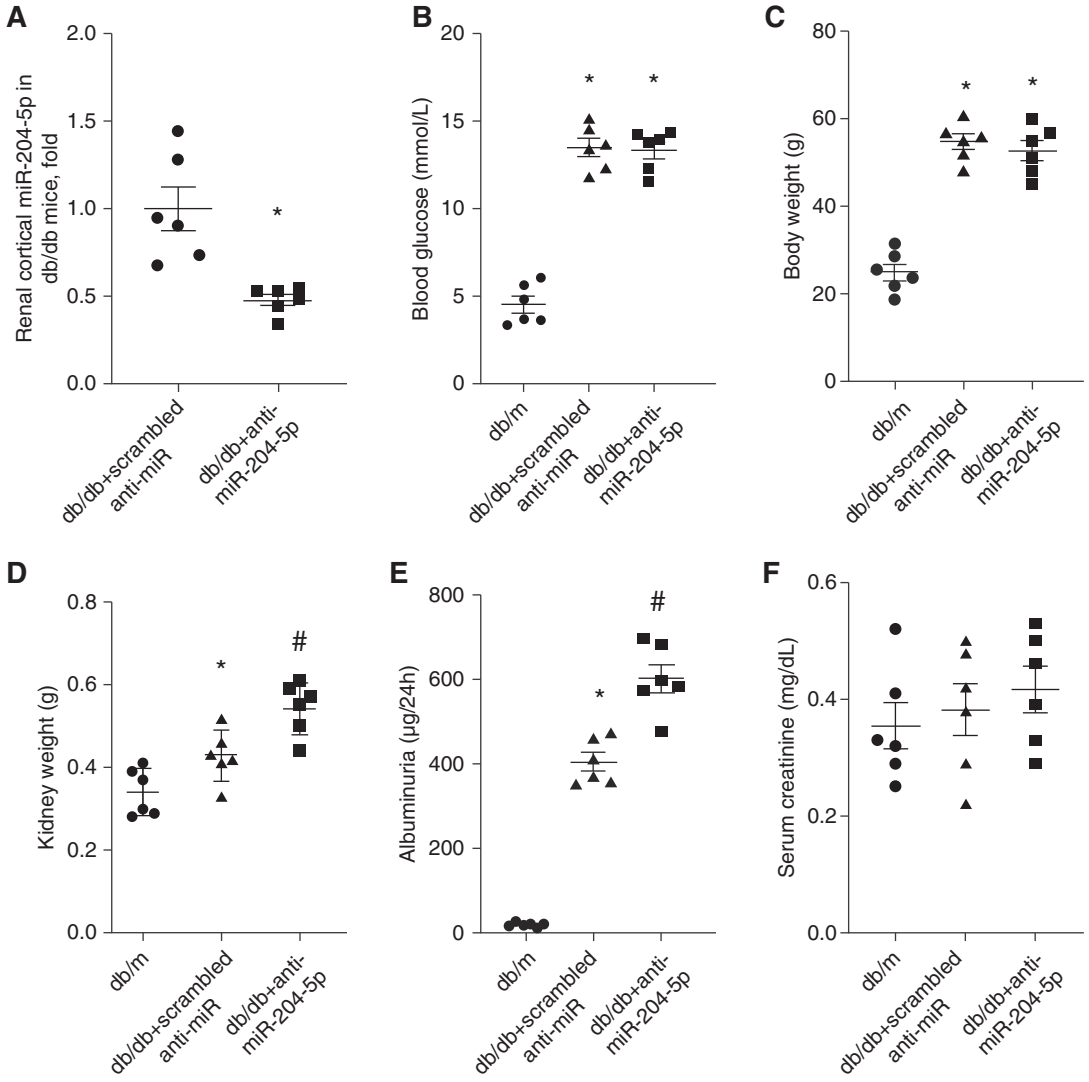


**Figure 7.** Treatment with anti-miR-204-5p exacerbates albuminuria in diabetic db/db mice without changing blood glucose. (A) miR-204-5p abundance, (B) Blood glucose, (C) body weight, (D) kidney weight, (E) urinary albumin, and (F) serum creatinine were measured in db/m mice and db/db mice treated with anti–miR-204-5p or control scrambled anti-miR for 12 weeks. $n=6$ for each group. $^{*}P<0.05$, versus db/m group and $^{\#}P<0.05$, versus scrambled anti-miR treatment, one-way ANOVA followed by Holm–Šidák test.

albuminuria whereas the treatment with anti–miR-204-5p further increased kidney weight and albuminuria in db/db mice (Figure 7, D and E). Serum creatinine level was not different between the groups (Figure 7F).

Renal fibrosis and mesangial matrix index were higher in db/db mice compared with control db/m mice (Figure 8, A–C). Treatment with anti–miR-204-5p resulted in significantly more fibrosis in renal cortical and outer medullary regions and higher mesangial matrix index in db/db mice compared with db/db mice treated with scrambled anti-miR. Consistent with these findings, the mRNA abundance of TGF-$\beta$1, COL1A1, monocyte chemoattractant protein-1, and P-selectin, fibrotic and inflammatory genes that are often upregulated in diabetic kidney injury,[10,36] were elevated in the renal cortex of db/db mice compared with db/m mice and further increased when db/db mice were treated with anti–miR-204-5p (Figure 8D). The mRNA and protein abundance of miR-204-5p target gene SHP2 and its downstream proinjurious effector, STAT3 activity, were higher in db/db mice compared with db/m mice and further increased in db/db/mice treated with anti–miR-204-5p (Figure 8, E and F). Similarly, SHP2 target and STAT3 regulator Src activity and mRNA abundance of SP1 and IL-6 receptor were higher in db/db mice and further increased by the anti–miR-204-5p treatment (Figure 8, G and H).

Lastly, we examined whether transfection with a miR-204-5p mimic would mitigate injurious responses in cultured mouse mesangial cells. Treatment with a high-glucose

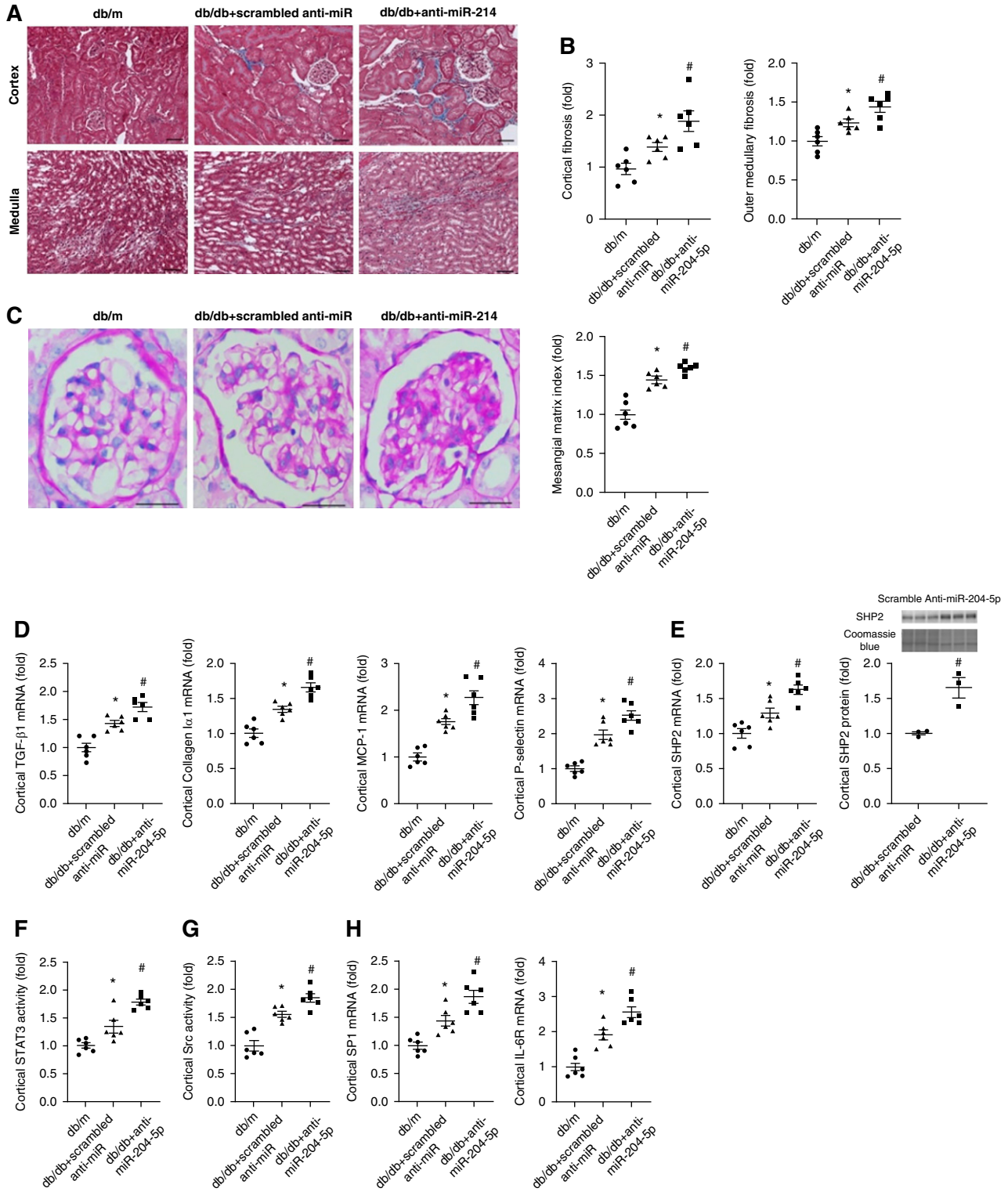


**Figure 8.** Treatment with anti–miR-204-5p exacerbates renal histologic injury and upregulates SHP2 in diabetic db/db mice. (A) Representative trichrome staining of kidney sections showing interstitial fibrosis (blue) in renal cortex and medulla in db/db mice after 12 weeks of treatment with anti–miR-204-5p or scrambled anti-miR. Scale bar, 100 $\mu$m; original magnification, ×200. (B) Semi-quantitative analysis of interstitial fibrosis shown in (A). (C) Representative periodic acid–Schiff staining of kidney sections showing mesangial expansion and extracellular matrix deposition and semiquantitative analysis in db/db mice after 12 weeks of treatment with anti–miR-204-5p or scrambled anti-miR. Scale bar, 50 $\mu$m; original magnification, ×400. (D) Cytokine or chemokine mRNA abundance,

medium significantly downregulated miR-204-5p in these cells (Supplemental Figure 1A). This response is different from the upregulation of miR-204-5p and the absence of change that we observed in the renal cortex of db/db mice and mice treated with uninephrectomy, Ang II, and salt, respectively. The finding suggests that miR-204-5p levels might change in a variety of ways depending on the specific injurious stimuli, the time course, or the tissue type involved. miR-204-5p abundance may change as an insufficient compensatory response in some cases but not others. The high-glucose treatment also increased collagen IV $\alpha$1 mRNA expression (Supplemental Figure 1B). Pretreatment with a miR-204-5p mimic significantly decreased collagen IV $\alpha$1 mRNA levels in cells treated with high glucose (Supplemental Figure 1B). This effect of miR-204-5p mimic was accompanied by downregulation of SHP2 protein and STAT3 activity (Supplemental Figure 1, C and D).

## DISCUSSION

This study demonstrates that endogenous miR-204 protects the kidneys against chronic renal injury induced by diabetes and hypertension, the two leading causes of ESKD. The presence of this new mechanism is supported by an analysis of human kidney biopsies, studies using miR-204-5p knockdown in a rat model, *Mir204* gene knockout in a mouse model, and miR-204-5p knockdown in diabetic db/db mice.

Several studies have shown a role for miR-204 in processes such as tissue development, cancer, light signaling, maintenance of epithelial phenotype, and insulin regulation.[47–51] miR-204 is the most highly expressed miRNA in the retinal pigment epithelium and maintains the integrity of the retinal pigment epithelium monolayer. This monolayer separates the photoreceptors and their choroidal blood supply and is fundamentally important for photoreceptor survival in diabetic retinopathy and age-related macular degeneration, a leading cause of blindness. A mutation in the seed region of miR-204 was reported to be responsible for inherited retinal dystrophy associated with ocular coloboma.[52]

miR-204 is also highly expressed in the kidney compared with other organs.[53,54] However, the functional role of miR-204 in chronic renal injury was unknown before this study. Results from this study indicate that the high abundance of miR-204 in the kidney is indeed functionally important in protecting the kidney against hypertensive and diabetic renal injury, two of the most common causes of chronic renal injury. This conclusion is supported by data from several distinct animal models of hypertensive and diabetic renal injury. Renal injury is worsened in *Mir204*$^{-/-}$ mice although the early phase of hypertension is attenuated. In other words, *Mir204* knockout does not exacerbate hypertension in our model of hypertension but it exacerbates renal injury. These findings highlight the prominent role of miR-204 as an inherent mechanism safeguarding the kidneys from the injurious effect of hypertension. Although both the -5p and -3p strands of miR-204 are lost in the knockout mice, the knockdown experiment in rats and db/db mice specifically targeted the -5p strand, which is also the strand significantly downregulated in human kidneys with hypertensive nephrosclerosis. These findings suggest the -5p strand is likely the functionally important strand of miR-204 in chronic renal injury.

The role of miR-204 in different types of hypertension and tissue injury may depend on etiology and the tissues involved. miR-204 attenuates pulmonary arterial remodeling and the development of pulmonary arterial hypertension.[40] On the other hand, miR-204 has been shown to promote endothelial dysfunction and vascular endoplasmic reticulum stress *via* downregulation of Sirtuin 1.[55] Our data indicate miR-204 might promote hypertension in the uninephrectomy, Ang II, and high-salt diet model but attenuate renal injury, including a mitigation of interlobular artery thickening, in multiple models. Interlobular artery thickening is a common pathologic finding in patients with hypertensive renal injury and may contribute to renal tissue hypoxia as the disease progresses. The protective effect of miR-204 on renal interlobular arteries may involve attenuation of vascular remodeling.

Targeting of SHP2 by miR-204-5p and the subsequent inhibition of STAT3 provide a plausible explanation for the protective effect of miR-204-5p against chronic renal injury. Interstitial inflammatory fibrosis is a major feature of chronic renal injury that leads to functional and morphologic deterioration of the kidney.[56,57] Activation of STAT3 is mitogenic and profibrotic in several tissues including the kidney.[41,43] SHP2 can activate Src and STAT3 and Src can activate STAT3.[40,58] miR-204-5p may protect the kidney from fibrotic injury by targeting SHP2 and suppressing the activation of STAT3. The miR-204–SHP2–STAT3 pathway may also influence chronic renal injury by regulating the renal vasculature.[59] Studies performed in pulmonary arterial smooth muscle cells have demonstrated that the downregulation of miR-204 accounts for the cell proliferation and resistance to apoptosis associated with pulmonary arterial hypertension.[40] The specific cell type mediating the effect of miR-204 on chronic renal injury remains to be identified, although the findings of this study suggest more than one cell type might be involved.

The miR-204–SHP2–STAT3 pathway may not the only pathway underlying the protective effect of miR-204 in

(E) SHP2 mRNA and protein abundance, (F) STAT3, and (G) Src activation measured by ELISA, and (H) SP1 and IL-6 receptor mRNA abundance in the renal cortex of db/db mice after 12 weeks of treatment with anti–miR-204-5p or scrambled anti-miR. $n=6$ for each group. $^{*}P<0.05$, versus db/m group and $^{\#}P<0.05$, versus scrambled anti-miR treatment, one-way ANOVA followed by Holm–Šidák test.

chronic renal injury. We did not observe any upregulation of SHP2 in *Mir204*$^{+/-}$ mice compared with wild-type littermates. Yet albuminuria and interlobular artery wall/lumen ratio were significantly increased in *Mir204*$^{+/-}$ mice. miR-204-5p can target genes other than SHP2. Downregulation of miR-204 was reported to enhance Runx2 expression and vascular smooth muscle cell calcification.[60] Wang *et al.*[61] showed that miR-204 targeted TGF-$\beta$ receptor 2 and SNAIL2. miR-204 targets Sirtuin 1 lysine deacetylase in the vasculature.[62] In fact, rather than being injurious, SHP2 might be protective against the signaling pathways downstream of Ang II–induced increases of reactive oxygen species in vascular smooth muscle cells.[63] In addition, STAT3 activation is regulated by several pathways in addition to SHP2. In future studies, it would be important to investigate the role of other target genes or pathways in the protective effect of miR-204 and how the targeting of SHP2 by miR-204-5p interacts with other pathways, including other miRNAs,[14] in the molecular regulatory networks that ultimately underlie the development and progression of chronic renal injury.

Pathophysiologic mechanisms of hypertensive and diabetic renal injury have several overlaps. The role of miR-204-5p might be part of the overlap. Downregulation of miR-204 has also been reported in advanced chronic allograft dysfunction and candidemia-induced kidney injuries.[15,64–67] These findings, together with the findings of this study, suggest broad relevance of miR-204 in kidney disease. It would be important to understand how the kidney maintains a higher level of miR-204 expression than other organs and how miR-204 expression is regulated in various types of renal injury in future studies.

## ACKNOWLEDGMENTS

M. Baker, Y. Cheng, B. Huang, J. Liu, X. Liu, Y. Liu, K. Usa, D. Wang, F. Wang, R. Wu, and J. Yin performed the experiments; Y. Cheng, M. Liang, J. Liu, and F. Wang drafted the paper; L. Dong, A. Geurts, S. Miller, and C. Zhang developed and maintained the knockout mouse model; Y. He, M. Liang, F. Wang, and N. Wang planned and led the study.

## DISCLOSURES

S. Miller has a patent (patent numbers 8710026 and 8455454) issued. All remaining authors have nothing to disclose.

## FUNDING

This study was supported by National Institutes of Health grants HL121233, HL125409, GM066730, and HL116264, and National Natural Science Foundation of China grants 81770741, 81570603, and 81400717.

## SUPPLEMENTAL MATERIAL

This article contains the following supplemental material online at http://jasn.asnjournals.org/lookup/suppl/doi:10.1681/ASN.2019101100/-/DCSupplemental.

Supplemental Table 1. Demographic and clinical characteristics of the human subjects with diabetic nephropathy and control subjects.

Supplemental Table 2. Sequences of custom-designed primers for real-time PCR.

Supplemental Figure 1. miR-204-5p mimic mitigates kidney cell injuries.

## REFERENCES

1. Atkins RC: The changing patterns of chronic kidney disease: the need to develop strategies for prevention relevant to different regions and countries. *Kidney Int Suppl* S83–S85, 2005
2. Jha V, Garcia-Garcia G: Global kidney disease - Authors' reply. *Lancet* 382: 1244, 2013
3. Lozano R, Gómez-Dantés H, Garrido-Latorre F, Jiménez-Corona A, Campuzano-Rincón JC, Franco-Marina F, et al.: [Burden of disease, injuries, risk factors and challenges for the health system in Mexico]. *Salud Publica Mex* 55: 580–594, 2013
4. Tervaert TW, Mooyaart AL, Amann K, Cohen AH, Cook HT, Drachenberg CB, et al.: Renal Pathology Society: Pathologic classification of diabetic nephropathy. *J Am Soc Nephrol* 21: 556–563, 2010
5. Kearney PM, Whelton M, Reynolds K, Muntner P, Whelton PK, He J: Global burden of hypertension: Analysis of worldwide data. *Lancet* 365: 217–223, 2005
6. Liang M, Liu Y, Mladinov D, Cowley AW Jr., Trivedi H, Fang Y, et al.: MicroRNA: A new frontier in kidney and blood pressure research. *Am J Physiol Renal Physiol* 297: F553–F558, 2009
7. Bartel DP: MicroRNAs: target recognition and regulatory functions. *Cell* 136: 215–233, 2009
8. Kozomara A, Griffiths-Jones S: miRBase: annotating high confidence microRNAs using deep sequencing data. *Nucleic Acids Res* 42: D68–D73, 2014
9. Phua YL, Ho J: MicroRNAs in the pathogenesis of cystic kidney disease. *Curr Opin Pediatr* 27: 219–226, 2015
10. Ninichuk V, Khandoga AG, Segerer S, Loetscher P, Schlapbach A, Revesz L, et al.: The role of interstitial macrophages in nephropathy of type 2 diabetic db/db mice. *Am J Pathol* 170: 1267–1276, 2007
11. Bhatt K, Kato M, Natarajan R: Mini-review: emerging roles of microRNAs in the pathophysiology of renal diseases. *Am J Physiol Renal Physiol* 310: F109–F118, 2016
12. Kriegel AJ, Mladinov D, Liang M: Translational study of microRNAs and its application in kidney disease and hypertension research. *Clin Sci (Lond)* 122: 439–447, 2012
13. Lorenzen JM, Haller H, Thum T: MicroRNAs as mediators and therapeutic targets in chronic kidney disease. *Nat Rev Nephrol* 7: 286–294, 2011
14. Liu Y, Taylor NE, Lu L, Usa K, Cowley AW Jr., Ferreri NR, et al.: Renal medullary microRNAs in Dahl salt-sensitive rats: miR-29b regulates several collagens and related genes. *Hypertension* 55: 974–982, 2010
15. Krupa A, Jenkins R, Luo DD, Lewis A, Phillips A, Fraser D: Loss of MicroRNA-192 promotes fibrogenesis in diabetic nephropathy. *J Am Soc Nephrol* 21: 438–447, 2010
16. Liu Y: Epithelial to mesenchymal transition in renal fibrogenesis: Pathologic significance, molecular mechanism, and therapeutic intervention. *J Am Soc Nephrol* 15: 1–12, 2004
17. Du B, Ma LM, Huang MB, Zhou H, Huang HL, Shao P, et al.: High glucose down-regulates miR-29a to increase collagen IV production in HK-2 cells. *FEBS Lett* 584: 811–816, 2010

18. Liu Y, Usa K, Wang F, Liu P, Geurts AM, Li J, et al.: MicroRNA-214-3p in the kidney contributes to the development of hypertension. *J Am Soc Nephrol* 29: 2518–2528, 2018
19. Baker MA, Davis SJ, Liu P, Pan X, Williams AM, Iczkowski KA, et al.: Tissue-specific MicroRNA expression patterns in four types of kidney disease. *J Am Soc Nephrol* 28: 2985–2992, 2017
20. Kriegel AJ, Liu Y, Cohen B, Usa K, Liu Y, Liang M: MiR-382 targeting of kallikrein 5 contributes to renal inner medullary interstitial fibrosis. *Physiol Genomics* 44: 259–267, 2012
21. Cowley AW Jr., Moreno C, Jacob HJ, Peterson CB, Stingo FC, Ahn KW, et al.: Characterization of biological pathways associated with a 1.37 Mbp genomic region protective of hypertension in Dahl S rats. *Physiol Genomics* 46: 398–410, 2014
22. Feng D, Yang C, Geurts AM, Kurth T, Liang M, Lazar J, et al.: Increased expression of NAD(P)H oxidase subunit p67(phox) in the renal medulla contributes to excess oxidative stress and salt-sensitive hypertension. *Cell Metab* 15: 201–208, 2012
23. Cowley AW Jr., Roman RJ, Kaldunski ML, Dumas P, Dickhout JG, Greene AS, et al.: Brown Norway chromosome 13 confers protection from high salt to consomic Dahl S rat. *Hypertension* 37: 456–461, 2001
24. Tian Z, Liu Y, Usa K, Mladinov D, Fang Y, Ding X, et al.: Novel role of fumarate metabolism in dahl-salt sensitive hypertension. *Hypertension* 54: 255–260, 2009
25. Xue H, Geurts AM, Usa K, Wang F, Lin Y, Phillips J, et al.: Fumarase overexpression abolishes hypertension attributable to endothelial NO synthase haploinsufficiency in dahl salt-sensitive rats. *Hypertension* 74: 313–322, 2019
26. Baker MA, Wang F, Liu Y, Kriegel AJ, Geurts AM, Usa K, et al.: MiR-192-5p in the kidney protects against the development of hypertension. *Hypertension* 73: 399–406, 2019
27. Song YH, Li Y, Du J, Mitch WE, Rosenthal N, Delafontaine P: Muscle-specific expression of IGF-1 blocks angiotensin II-induced skeletal muscle wasting. *J Clin Invest* 115: 451–458, 2005
28. Nishijima Y, Zheng X, Lund H, Suzuki M, Mattson DL, Zhang DX: Characterization of blood pressure and endothelial function in TRPV4-deficient mice with l-NAME- and angiotensin II-induced hypertension. *Physiol Rep* 2: e00199, 2014
29. Tian Z, Greene AS, Pietrusz JL, Matus IR, Liang M: MicroRNA-target pairs in the rat kidney identified by microRNA microarray, proteomic, and bioinformatic analysis. *Genome Res* 18: 404–411, 2008
30. Liang M, Yuan B, Rute E, Greene AS, Olivier M, Cowley AW Jr.: Insights into Dahl salt-sensitive hypertension revealed by temporal patterns of renal medullary gene expression. *Physiol Genomics* 12: 229–237, 2003
31. Liu Y, Park F, Pietrusz JL, Jia G, Singh RJ, Netzel BC, et al.: Suppression of 11beta-hydroxysteroid dehydrogenase type 1 with RNA interference substantially attenuates 3T3-L1 adipogenesis. *Physiol Genomics* 32: 343–351, 2008
32. Liang M, Pietrusz JL: Thiol-related genes in diabetic complications: a novel protective role for endogenous thioredoxin 2. *Arterioscler Thromb Vasc Biol* 27: 77–83, 2007
33. Mori T, Polichnowski A, Glocka P, Kaldunski M, Ohsaki Y, Liang M, et al.: High perfusion pressure accelerates renal injury in salt-sensitive hypertension. *J Am Soc Nephrol* 19: 1472–1482, 2008
34. Mori T, Cowley AW Jr.: Role of pressure in angiotensin II-induced renal injury: Chronic servo-control of renal perfusion pressure in rats. *Hypertension* 43: 752–759, 2004
35. Huang B, Cheng Y, Usa K, Liu Y, Baker MA, Mattson DL, et al.: Renal tumor necrosis factor $\alpha$ contributes to hypertension in dahl salt-sensitive rats. *Sci Rep* 6: 21960, 2016
36. Wu R, Liu X, Yin J, Wu H, Cai X, Wang N, et al.: IL-6 receptor blockade ameliorates diabetic nephropathy via inhibiting inflammasome in mice. *Metabolism* 83: 18–24, 2018
37. Cowley AW Jr., Roman RJ: The role of the kidney in hypertension. *JAMA* 275: 1581–1589, 1996
38. Rapp JP: Genetic analysis of inherited hypertension in the rat. *Physiol Rev* 80: 135–172, 2000
39. Lu L, Li P, Yang C, Kurth T, Misale M, Skelton M, et al.: Dynamic convergence and divergence of renal genomic and biological pathways in protection from Dahl salt-sensitive hypertension. *Physiol Genomics* 41: 63–70, 2010
40. Courboulin A, Paulin R, Giguère NJ, Saksouk N, Perreault T, Meloche J, et al.: Role for miR-204 in human pulmonary arterial hypertension. *J Exp Med* 208: 535–548, 2011
41. Pang M, Ma L, Gong R, Tolbert E, Mao H, Ponnusamy M, et al.: A novel STAT3 inhibitor, S3I-201, attenuates renal interstitial fibroblast activation and interstitial fibrosis in obstructive nephropathy. *Kidney Int* 78: 257–268, 2010
42. Yan Y, Ma L, Zhou X, Ponnusamy M, Tang J, Zhuang MA, et al.: Src inhibition blocks renal interstitial fibroblast activation and ameliorates renal fibrosis. *Kidney Int* 89: 68–81, 2016
43. Bienaimé F, Muorah M, Yammine L, Burtin M, Nguyen C, Baron W, et al.: Stat3 controls tubulointerstitial communication during CKD. *J Am Soc Nephrol* 27: 3690–3705, 2016
44. Thomas KR, Capecchi MR: Site-directed mutagenesis by gene targeting in mouse embryo-derived stem cells. *Cell* 51: 503–512, 1987
45. Zhang J, Patel MB, Griffiths R, Mao A, Song YS, Karlovich NS, et al.: Tumor necrosis factor-$\alpha$ produced in the kidney contributes to angiotensin II-dependent hypertension. *Hypertension* 64: 1275–1281, 2014
46. Zhang JD, Patel MB, Song YS, Griffiths R, Burchette J, Ruiz P, et al.: A novel role for type 1 angiotensin receptors on T lymphocytes to limit target organ damage in hypertension. *Circ Res* 110: 1604–1617, 2012
47. Volinia S, Galasso M, Costinean S, Tagliavini L, Gamberoni G, Drusco A, et al.: Reprogramming of miRNA networks in cancer and leukemia. *Genome Res* 20: 589–599, 2010
48. Krol J, Busskamp V, Markiewicz I, Stadler MB, Ribi S, Richter J, et al.: Characterizing light-regulated retinal microRNAs reveals rapid turnover as a common property of neuronal microRNAs. *Cell* 141: 618–631, 2010
49. Conte I, Carrella S, Avellino R, Karali M, Marco-Ferreres R, Bovolenta P, et al.: miR-204 is required for lens and retinal development via Meis2 targeting. *Proc Natl Acad Sci U S A* 107: 15491–15496, 2010
50. Xu G, Chen J, Jing G, Shalev A: Thioredoxin-interacting protein regulates insulin transcription through microRNA-204. *Nat Med* 19: 1141–1146, 2013
51. Hall DP, Cost NG, Hegde S, Kellner E, Mikhaylova O, Stratton Y, et al.: TRPM3 and miR-204 establish a regulatory circuit that controls oncogenic autophagy in clear cell renal cell carcinoma. *Cancer Cell* 26: 738–753, 2014
52. Conte I, Hadfield KD, Barbato S, Carrella S, Pizzo M, Bhat RS, et al.: MiR-204 is responsible for inherited retinal dystrophy associated with ocular coloboma. *Proc Natl Acad Sci U S A* 112: E3236–E3245, 2015
53. Liang Y, Ridzon D, Wong L, Chen C: Characterization of microRNA expression profiles in normal human tissues. *BMC Genomics* 8: 166, 2007
54. Sun Y, Koo S, White N, Peralta E, Esau C, Dean NM, et al.: Development of a micro-array to detect human and mouse microRNAs and characterization of expression in human organs. *Nucleic Acids Res* 32: e188, 2004
55. Kassan M, Vikram A, Kim YR, Li Q, Kassan A, Patel HH, et al.: Corrigendum: Sirtuin1 protects endothelial Caveolin-1 expression and preserves endothelial function via suppressing miR-204 and endoplasmic reticulum stress. *Sci Rep* 7: 46123, 2017
56. Meyrier A: Nephrosclerosis: A term in quest of a disease. *Nephron* 129: 276–282, 2015
57. Hill GS: Hypertensive nephrosclerosis. *Curr Opin Nephrol Hypertens* 17: 266–270, 2008
58. Fornaro M, Burch PM, Yang W, Zhang L, Hamilton CE, Kim JH, et al.: SHP-2 activates signaling of the nuclear factor of activated T cells to promote skeletal muscle growth. *J Cell Biol* 175: 87–97, 2006

59. Bidani AK, Polichnowski AJ, Loutzenhiser R, Griffin KA: Renal microvascular dysfunction, hypertension and CKD progression. *Curr Opin Nephrol Hypertens* 22: 1–9, 2013
60. Cui RR, Li SJ, Liu LJ, Yi L, Liang QH, Zhu X, et al.: MicroRNA-204 regulates vascular smooth muscle cell calcification *in vitro* and *in vivo*. *Cardiovasc Res* 96: 320–329, 2012
61. Wang FE, Zhang C, Maminishkis A, Dong L, Zhi C, Li R, et al.: MicroRNA-204/211 alters epithelial physiology. *FASEB J* 24: 1552–1571, 2010
62. Vikram A, Kim YR, Kumar S, Li Q, Kassan M, Jacobs JS, et al.: Vascular microRNA-204 is remotely governed by the microbiome and impairs endothelium-dependent vasorelaxation by downregulating Sirtuin1. *Nat Commun* 7: 12565, 2016
63. Tabet F, Schiffrin EL, Callera GE, He Y, Yao G, Ostman A, et al.: Redox-sensitive signaling by angiotensin II involves oxidative inactivation and blunted phosphorylation of protein tyrosine phosphatase SHP-2 in vascular smooth muscle cells from SHR. *Circ Res* 103: 149–158, 2008
64. Li XY, Zhang K, Jiang ZY, Cai LH: MiR-204/miR-211 downregulation contributes to candidemia-induced kidney injuries via derepression of Hmx1 expression. *Life Sci* 102: 139–144, 2014
65. Munari E, Marchionni L, Chitre A, Hayashi M, Martignoni G, Brunelli M, et al.: Clear cell papillary renal cell carcinoma: micro-RNA expression profiling and comparison with clear cell renal cell carcinoma and papillary renal cell carcinoma. *Hum Pathol* 45: 1130–1138, 2014
66. Koller K, Pichler M, Koch K, Zandl M, Stiegelbauer V, Leuschner I, et al.: Nephroblastomas show low expression of microR-204 and high expression of its target, the oncogenic transcription factor MEIS1. *Pediatr Dev Pathol* 17: 169–175, 2014
67. Scian MJ, Maluf DG, David KG, Archer KJ, Suh JL, Wolen AR, et al.: MicroRNA profiles in allograft tissues and paired urines associate with chronic allograft dysfunction with IF/TA. *Am J Transplant* 11: 2110–2122, 2011

## AFFILIATIONS

[1]Department of Nephrology, Shenzhen Second People's Hospital, First Affiliated Hospital of Shenzhen University, Clinical Institute of Anhui Medical University, Shenzhen, People's Republic of China
[2]The Center for Nephrology and Urology, Shenzhen University Health Science Center, Shenzhen University, Shenzhen, People's Republic of China
[3]Center of Systems Molecular Medicine, Department of Physiology, Medical College of Wisconsin, Milwaukee, Wisconsin
[4]Department of Nephrology, Shenzhen Traditional Chinese Medicine Hospital, The Fourth Clinical Medical College of Guangzhou University of Chinese Medicine, Shenzhen, People's Republic of China
[5]Department of Nephrology, Shanghai Jiao Tong University Affiliated Sixth People's Hospital, Shanghai, People's Republic of China
[6]Division of Nephrology, Department of Medicine, Medical College of Wisconsin, Milwaukee, Wisconsin
[7]Section of Epithelial and Retinal Physiology and Disease, National Eye Institute, National Institutes of Health, Bethesda, Maryland
[8]Department of Nephrology, Shenzhen Hengsheng Hospital, Shenzhen, Guangdong, People's Republic of China